A more than 20 Mrad/s speed RSOP monitoring method with large PMD tolerance in optical coherent communication systems

Linan Shan, Xiaoguang Zhang*, Peng Sun, Guanghao Yao, Wanxin Zhao, Lixia Xi, Xiaosheng Xiao
State Key Laboratory of Information Photonics and Optical Communications, School of Electronic Engineering, Beijing University of Posts and Telecommunications (BUPT), Beijing 100876, China
xgzhang@bupt.edu.cn

Abstract: We propose a RSOP monitoring method, integrated in DSP of the coherent receiver, which can reach the RSOP speed of more than 20Mrad/s with tolerance for residual CD and large PMD along with second PMD.

1. Introduction

In optical fiber communication system, some severe fiber risk events, like fiber bending and shaking, and even the lightning strike, are connected with the fast rotation of state-of-polarization (RSOP). Therefore, it is important to monitor the RSOP in fiber link, especially for the polarization multiplexing system. In a coherent fiber communication system, several methods were proposed to monitor the RSOP by analyzing the adaptive coefficients of the MIMO algorithms such as CMA integrated in the DSP of the coherent receiver [1, 2]. However, these MIMO algorithms cease to be effective when the RSOP speed reaches more than several mega rad/s [3], or only several hundred-kilo rad/s if accompanied with polarization mode dispersion (PMD).

In this paper, we propose a new RSOP monitoring method which can monitor more than 20 Mrad/s RSOP, based on the wavelet transformation analysis of polarization tributary power, with enough residual chromatic dispersion (rCD) tolerance of 50 ps/nm after the CD compensation module in DSP of the receiver, and very large PMD tolerance, as large as 180 ps differential group delay (DGD), with the second PMD tolerance as large as 340 ps^2.

2. Principle of RSOP monitoring

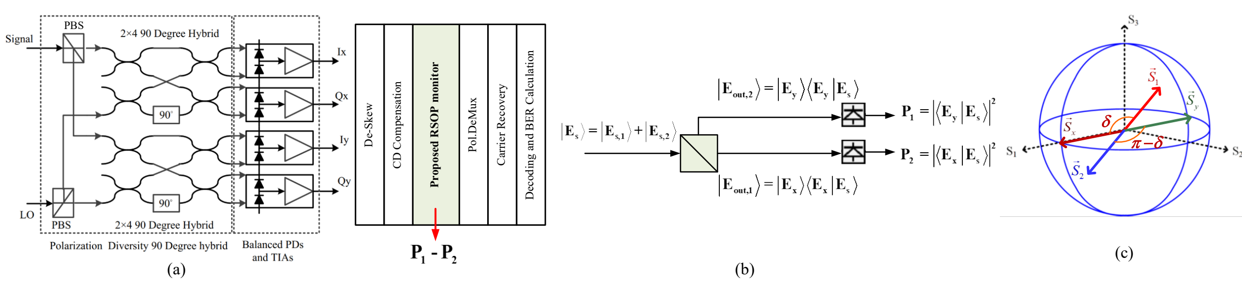

Fig. 1 The structure diagram of the proposed RSOP monitoring

Figure 1 illustrates the proposed RSOP monitoring method integrated in the DSP of the coherent receiver. The monitoring module is located between the modules of CD compensation and polarization de-multiplexing, as shown in Fig.1(a). The equivalent structure of monitoring is drawn in Fig.1(b). At the receiver end, the signal vector $|\mathbf{E}_s\rangle$ is denoted by $|\mathbf{E}_s\rangle = |\mathbf{E}_{s,1}\rangle + |\mathbf{E}_{s,2}\rangle$, where $|\mathbf{E}_{s,1}\rangle$ and $|\mathbf{E}_{s,2}\rangle$ are the two signals in orthogonal polarization tributaries. The polarization beam splitter (PBS) makes the projection of the signal vector $|\mathbf{E}_s\rangle$ onto the eigenvectors $|\mathbf{E}_x\rangle$ and $|\mathbf{E}_y\rangle$ of PBS, and we get the two signal outputs $|\mathbf{E}_{out,1}\rangle = |\mathbf{E}_x\rangle\langle\mathbf{E}_x|\mathbf{E}_s\rangle$ and $|\mathbf{E}_{out,2}\rangle = |\mathbf{E}_y\rangle\langle\mathbf{E}_y|\mathbf{E}_s\rangle$, and also get two power outputs P_1 and P_2. In Fig.1(c), the polarization state vectors $\vec{S}_1(t)$ and $\vec{S}_2(t)$ changing with time in Stokes space correspond to the signals $|\mathbf{E}_{s,1}\rangle$ and $|\mathbf{E}_{s,2}\rangle$. Also, the $\vec{S}_x$ and $\vec{S}_y$ correspond to two fixed eigenvectors $|\mathbf{E}_x\rangle$ and $|\mathbf{E}_y\rangle$. $\vec{S}_1$ is at the anti-direction of $\vec{S}_2$, and the same for $\vec{S}_x$ and $\vec{S}_y$. The angles between $\vec{S}_1(t)$ and $\vec{S}_x$, $\vec{S}_2(t)$ and $\vec{S}_y$ are $\delta(t)$ and $\pi-\delta(t)$, respectively, as shown in Fig.1(c). It is proved that the time average of two power outputs $\overline{P_1 - P_2}$ is

$$P(t) = \overline{P_1 - P_2} = P_0 \sin\delta(t) \tag{1}$$

In short, in DSP we can calculate $P(t)$, which reflects the frequency features of the projection angle change $\delta(t)$, and hence it indicates the polarization change in Stokes space. Therefore, we can use short time Fourier transformation (STFT) or wavelet transformation to extract the frequency feature of RSOP from $P(t)$. We make the wavelet transformation of $P(t)$ and obtain polarization change frequency WT_f [4]. The RSOP speed is $2\pi \times WT_f$ in rad/s.

3. Experimental verification and analysis

According to the experimental block diagram in Fig.2(a), the laser (NEO ECL1994) emits a laser light with a line-width of 100 kHz, and center wavelength of 1550 nm. The 112 GBaud optical PDM-16QAM signal is generated by the arbitrary wave generator and the dual-polarization IQ modulator. The signal light then enters the scrambler (EPS1000), in which we use the half-wave-plate (HWP) scrambling mode to generate the RSOP with a scrambling speed of 20 Mrad/s. The PMD emulator (PMD-1000) is behind the scrambler, which can emulate the PMD up to second order. The parameter settings of the DGD and second PMD are shown in Table 1. The second and third rows in Table 1 give the values the first-order mean PMD (1st PMD), and the second-order mean PMD (2nd PMD). After the PMD emulator, the optical signal enters a 3 km fiber and EDFA. Here 3 km standard single mode fiber offers the chromatic dispersion of about 50 ps/nm, which represents the residual CD after the CD compensation in the DSP receiver. Then the transmitted signals are received using the coherent receiver which is the combination of a pol-diversity optical hybrid with a real-time oscilloscope at the sampling rate of 153.6GSa/s, as shown in Fig.2(b). We use an average of 2000 received signal to extract the polarization variation. Then, the offline processing gets the RSOP speed using the method described in section 2.

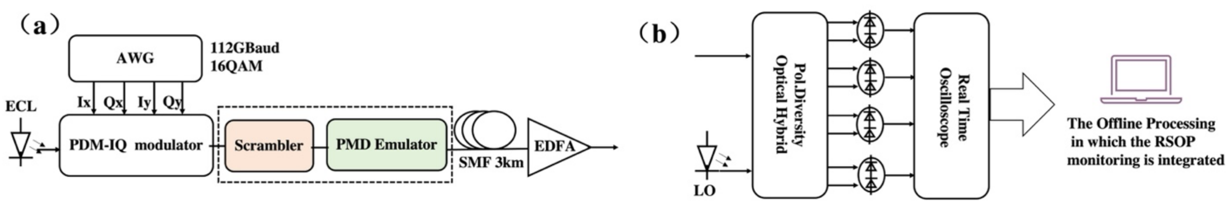

Fig. 2. (a) The transmitter and transmission diagram. (b) The receiver and monitoring diagram.

Table 1. The parameter settings for the PMD Emulator (PMD-1000)

ID	2	4	8	…	63	255	257	261	270	…	555	642
1st PMD/ps	1.79	3.21	6.07	…	45.34	182.4	1.47	3.05	5.984	…	59.99	74.4
2nd PMD/ps^2	0	0	0	…	0	0	0.5	3.059	10.19	…	64.2	344.5

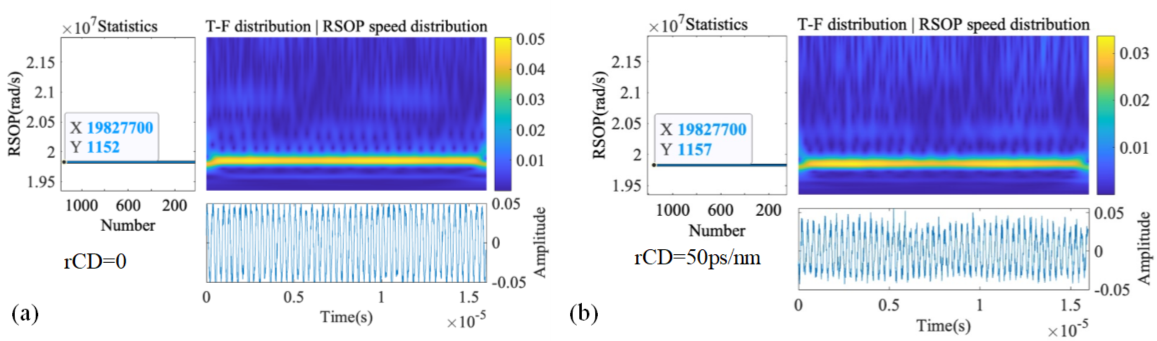

Fig. 3. (a) RSOP monitoring results without considering CD and PMD. (b) The result considering the impact of rCD.

Because the aim of this experiment is only to monitor the RSOP instead of getting equalized received signal, we only make the modules of De-skew and orthonormalization, clock recovery in service, with the other equalization modules out of work such as CD compensation, polarization de-multiplexing, etc. At first, we evaluate the RSOP monitoring without PMD emulator and 3 km fiber. The results are shown in Fig. 3 (a), where the bottom row shows the variation of $P(t)$, and the upper row gives the wavelet transformation of $P(t)$ in 2-D manner and its variation with time in 3-D manners. We can see that the proposed method obtains almost the exact value of 20 Mrad/s RSOP (the main frequency component is at 19.8 Mrad/s, with a monitoring error less than 1%), and almost the same speed within 16 μs. Then using 3 km fiber, Fig. 3(b) shows the 50 ps/nm residual CD does an impact to the contrast ratio of $P(t)$, but little impact to RSOP speed, which means the proposed method has enough rCD tolerance in a coherent fiber transmission system.

When considering the impact of both rCD of 50 ps/nm and PMD, we also evaluate the monitoring performance of the proposed method. At first, we consider only the impact of 1st PMD, as shown in Fig.4(a) and (b). Compared with Fig. 3(b) without PMD, here we take 1.79 ps 1st PMD into account. Therefore, we observe that the contrast ratio of $P(t)$ is further reduced, but the RSOP monitoring accuracy is not much deteriorated (as shown in Fig. 4(a)) by the 1st PMD up to 180 ps (in Fig. 4(b)). However, when we take the 2nd PMD into account, for example 344 ps^2, the contrast ratio of $P(t)$ is severely reduced, leading to a somewhat indistinct frequency feature of $P(t)$, with the result that monitoring accuracy decreased (as shown in Fig. 4(c)). We can further find that the clear contrast ratio of $P(t)$ or the distinct frequency feature of $P(t)$ is the key to maintain the performance of the proposed RSOP monitoring method. The modest rCD and large 1st PMD do not severely degrade distinct frequency feature of $P(t)$, and this is the reason why the proposed method has rCD and PMD tolerance.

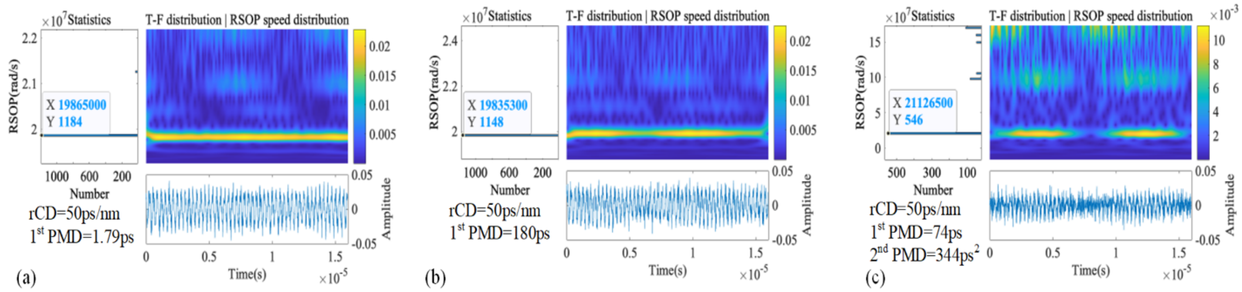

Fig. 4. Performance of proposed monitor at 20Mrad/s polarization change with rCD 50ps/nm and different values of PMD. (a)1st PMD 1.79ps. (b)1st PMD 182.4ps. (c) 1st PMD 74 ps + 2nd PMD 344.5ps^2.

Figure 5 depicts the impacts of only 1st PMD and 1st PMD + 2nd PMD on the RSOP monitoring performance, combined with the effect of 50 ps/nm rCD. We can see that: for only 1st PMD the monitoring errors are all smaller than 2%, for the DGD range from 1.79 to 180 ps, as shown in Fig. 5(a); And for the case of 1st PMD + 2nd PMD, in a large range of 1.47 ps + 0.50 ps^2, to 44.98 ps + 16.00 ps^2, the monitoring error is still under the value of 2%. Only in the severe case of 59.99 ps + 64.20 ps^2 and 74.40 + 344.50 ps^2, the monitoring errors reach 4% and 5%, which are still tolerable. Note that the monitoring RSOP speed can be larger than 20 Mrad/s, and here it is limited by the maximum speed of the scrambler used. Furthermore, random variation of RSOP can also be monitored by the proposed method, and the experimental data is not shown here due to the limited space. This ultra-fast monitoring speed and large tolerance of PMD and CD mean that the proposed method is sufficient for monitoring transient polarization changes caused by extreme fiber events, such as mechanical vibration and even lightning strikes [5].

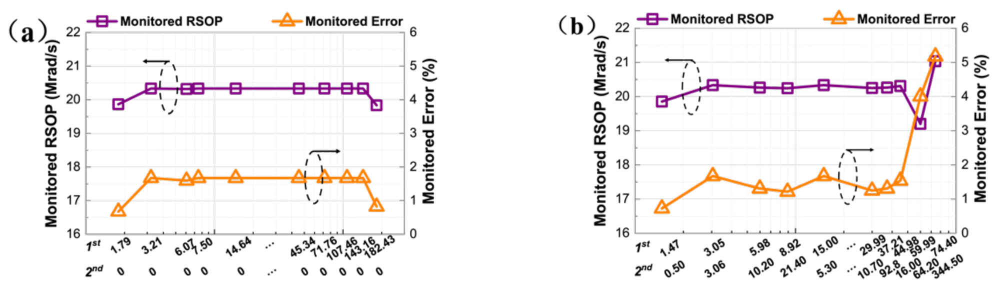

Fig. 5. The monitoring performance under the RSOP speed 20 Mrad/s. (a) The monitoring tolerance for only 1st PMD. (b) The results for the combination of 1st PMD + 2nd PMD.

4. Conclusion

We proposed a new ultra-high speed RSOP monitoring method with tolerance for CD and large PMD up to second order.

This work is partly supported by the National Science Foundation of China (62071065, 62101062).

5. Reference

[1] Y. Qi, et al., Proc. OECC, TuB2-4 (2019).
[2] T. Ye, et al., Proc. OFC, M4I.1 (2019).
[3] J. Li, et al., Proc. ECOC (2021), pp. 1-4.
[4] S. Qian, "Introduction to Time-Frequency and Wavelet Transforms," (2001), pp. 1-4.
[5] R. Noe, et al., Photonic Networks; 19th ITG-Symposium, (2018), pp. 1-4.